A phase Ib/IIa randomized trial of Enoxacin in patients with ALS

Iddo Magen[1,2], Hannah Marlene Kaneb[3], Maria Masnata[3], Nisha Pulimood[3], Anna Emde[1,2], Angela Genge[3*], Eran Hornstein[1,2#]

1 Department of Molecular Genetics, Weizmann Institute of Science

2 Department of Molecular Neuroscience, Weizmann Institute of Science

3 Montreal Neurological Institute-Hospital, McGill University, Montreal, Canada.

* Corresponding author for clinical research

#Corresponding author for molecular research

Correspondence to:

Angela Genge, Montreal Neurological Institute and Hospital, Department of Neurology, 3801 University Street, Suite 207, Montreal, QC, CA H3A 2B4, email: angela.genge@mcgill.ca

Eran Hornstein, Arnold R. Meyer Building, Room 313, Weizmann Institute of Science, Rehovot 76100, Israel, email: eran.hornstein@weizmann.ac.il

Abstract

Background and Objectives: The RNAse III DICER is essential for miRNA biogenesis. DICER activity is downregulated in sporadic and genetic forms of ALS. Accordingly, hundreds of miRNAs are broadly downregulated, and their mRNA targets are de-repressed. Enoxacin is a fluoroquinolone, which increases DICER activity and miRNA biogenesis. In an investigator-initiated, first-in-patient phase Ib/IIa study, we tested Enoxacin safety and tolerability in patients with ALS and explored pharmacodynamic biomarkers for Enoxacin target engagement.

Trial design: REALS1 was a randomized, double-blind, parallel group study.

Methods: Patients with sporadic ALS who met inclusion criteria were dosed with 200mg, 400mg or 600mg oral Enoxacin twice daily for 30 days. Randomization was conducted as per a randomization sequence generated by the study statistician. The study participants, care givers, and those assessing outcomes were blinded to dose assignment throughout the study. The main objective of this trial was safety and tolerability, and primary outcomes were the number and severity of adverse events and number of patients completing dosing. Other objective was pharmacodynamic biomarkers for Enoxacin target engagement, measured by profiling miRNAs by RNA-seq.

Results: A total of eight patients were randomized to either 200mg x 2/day (n=3), 400mg x 2/day (n=3) or 600mg x 2/day (n=2). Patients did not experience any serious adverse events. One patient in the 600 mg x 2/day group discontinued the study early, due to adverse events that were not life-threatening. Molecular analysis of cell-free miRNA in plasma and CSF was performed in the 200mg x 2/day and 400mg x 2/day groups, in which all patients completed dosing. This analysis revealed a global increase in plasma and CSF miRNA levels in all post-treatment time points, compared to baseline.

Conclusion: Enoxacin is safe and tolerable and provides important evidence for in-patient target engagement. These results encourage testing Enoxacin efficacy in larger trials.

Trial Registration information: ClinicalTrials.gov identifier: NCT04840823. Submitted on March 29, 2021. First patient enrolled on April 8, 2021.

Funding: ALS Association, ALS Canada, eRARE FP7, Israel Ministry of Health, Muscular Dystrophy Canada, Canadian Institutes of Health Research and Fonds de recherche du Québec - Santé.

Introduction

Amyotrophic lateral sclerosis (ALS) is a devastating neurodegenerative syndrome of the human motor neuron system(1). Except for Tofersen therapy for SOD1-ALS (2), disease-modifying treatments do not exist. Studies over the last 20 years have uncovered ALS-causing mutations in a number of genes(3), many of which code for RNA-binding proteins (e.g. TDP-43, HNRNP A2/B1, HNRNP A1 and FUS). It is therefore hypothesized that dysregulation of RNA activity may be involved in the pathogenesis of ALS (4-8). Accordingly, dysregulated splicing has been recently suggested to play an important role in pathogenesis because of the loss of normal TDP-43(9-12). However, other facets of RNA dysregulation are not fully explored.

microRNAs (miRNAs) are endogenous non-protein-coding small RNAs. miRNAs silence messenger RNA (mRNA) expression by degradation and translational inhibition. The involvement of miRNAs in ALS pathogenesis is suggested by a global downregulation of miRNAs in motor neurons of patients with ALS (13-16).

DICER is an RNAse III, which works in concert with TDP-43 to promote miRNA biogenesis (17). DICER cleaves the precursor miRNAs (pre-miRNAs), giving rise to single-stranded mature miRNAs (18). Stress and the expression of ALS-causing mutant forms of TDP-43, FUS or SOD1, resulted in inhibition of DICER activity and accumulation of pre-miRNA species (14). Consistently, spinal motor neuron-specific knockout of Dicer in adult mice resulted in progressive loss of motor neurons, denervation, and muscular atrophy (4).

While almost all miRNAs are dependent on DICER for their biogenesis and function, miR-451a is Dicer independent as it is processed by Argonaute protein (Ago2) (19). Importantly, Dicer-dependent miRNAs compete with miR-451a in binding to the effector complex, RISC. Therefore, an increase in DICER activity results in relative upregulation of mature miRNAs and relative depletion of miR-451 (20).

Enoxacin is a fluoroquinolone anti-bacterial drug that was identified as an agonist of DICER complex activity, via increasing the binding of pre-miRNAs(21-23). Enoxacin elevated miRNA levels in rat frontal cortex (24) and rescued expression of miRNAs that were

downregulated by ALS-associated mutations in cell line (14) and in iPSC-derived motor neurons (25). Enoxacin also promoted assembly of paraspeckles which are protective in neuroblastoma cells with compromised microRNA/dsRNA metabolism (26). This suggests that the general upregulation of miRNA levels can be beneficial by regulating key genes that modulate pathological phenotypes. Furthermore, Enoxacin mitigated some of the symptoms associated with motor deterioration in the SOD1G93A and TDP-43A315T ALS mouse models (14). These preclinical data support the potential use of Enoxacin as a novel disease-modifying drug and prompted us to initiate a study of Enoxacin safety and tolerability in patients with ALS.

Cell-free miRNAs are studied as potential biomarkers in neurodegeneration (25, 27-58). Accordingly, we have recently shown that circulating miR-181 can serve as an ALS prognostication biomarker (59), and that miRNAs can predict the response to Spinraza therapy in spinal muscular atrophy (60) and assist the diagnosis of frontotemporal dementia(61). Therefore, we hypothesized that cell-free miRNAs might also serve pharmacodynamic analysis and could potentially reveal the engagement of Enoxacin onto its therapeutic target, DICER, in human participants.

Here, we report the findings from a phase Ib/IIa study of orally administered Enoxacin in people with ALS. We demonstrate that Enoxacin is safe and tolerable. As a support for target engagement, we found that Enoxacin globally increases miRNA levels in the plasma and the CSF and that the magnitude of the molecular changes in miRNAs is associated with the concentration of Enoxacin in the plasma. Thus, our study encourages further studies to assess the efficacy of Enoxacin in patients with ALS.

Materials and Methods

Trial design and oversight

REALS1 (ClinicalTrials.gov identifier: NCT04840823) was a randomized, double-blind, parallel groups, phase 1b/2a study of Enoxacin in patients with ALS. It assessed the safety and tolerability of Enoxacin, which was dosed orally at 400mg, 800mg or 1200mg per day, in adults with ALS. The study protocol was approved by the Research Ethics Board at MNI (CRU / 2020-6359). The study enrolled participants at Montreal Neurological Institute (MNI), Quebec, Canada from April 2021 through March 2023. All participants provided written informed consent. Participants were evaluated and monitored in the clinic on days 1, 7, 14, 21, and 30 of treatment and at a follow-up visit 14 days after the last dose.

Sample size determination

The determination of sample size for this study was limited by its exploratory nature. This study was a small, early-phase study to assess dose range and design in preparation for a large-scale study in the future. There was no effect size available for calculation at the time the protocol was written. The investigators decided that 36 patients (12 per treatment arm) would be adequate for the initial assessment of safety, tolerability, PK, and PD of three doses of enoxacin in adults with ALS. However, the number of recruited patients was dramatically affected by restrictions due to COVID and the burden the pandemic imposed, particularly on the participation of Canadian patients with ALS in a full 30-day study in Montreal Neurological Institute.

Participant inclusion criteria

Participants were diagnosed with either familial or sporadic ALS and were on a stable dose of Riluzole for at least 30 days prior to screening. Participants with a forced vital capacity (FVC) lower than 50% of what is expected by age, height, weight, and sex were excluded. reported hypersensitivity/allergy to fluoroquinolone was an exclusion criterion. Diagnosis of an additional neurodegenerative disease, pulmonary disorder not attributed to ALS, severe renal impairment or impaired liver function also resulted in exclusion. Patients currently enrolled in another clinical trial involving an experimental drug or device were excluded as well.

Randomization and blinding

Patients were randomly allocated to one of the dosing groups and were administered with a single morning dose and a single evening dose of Enoxacin for 30 days (Figures 1, 2). A single morning dose (200mg, 400mg or 600mg) was administered on days 1 and 30 to determine Enoxacin pharmacokinetics (Cmax, Tmax) over 24 hours.

The study statistician generated a random allocation sequence, enrolled participants, and randomly assigned them to interventions as per the sequence. Block randomization with block size of 3 was used to achieve balance and maintain the blind. The study statistician and a delegated individual not involved in the day to day running of the study were unblinded to the randomization code for the purposes of the generation and verification of this code, however they had no contact with study participants and were unaware of the identity of the study participants, whose treatment were assigned based on this allocation sequence.

The sponsor, study participants, principal investigators, coordinators, clinical laboratory staff and all other study site staff except for the study pharmacist(s), were blinded to participant treatment dose assignment throughout the study. To preserve blinding, an identical placebo tablet composed of excipient only was provided to patients assigned to doses that did not require 3 ‘active’ 200mg Enoxacin tablets to complete one dose. Thus, patients receiving 200mg Enoxacin x 2 / day took one 200mg Enoxacin tablet and two placebo tablets twice daily, patients receiving 400mg x 2/day took two 200mg Enoxacin tablets and one placebo tablet twice daily, and patients receiving 600mg x2/day took three Enoxacin tablets twice daily. Enoxacin and placebo tablets were in-kind gifts from Apotex, Inc., Toronto, Canada.

Study endpoints

The primary endpoints evaluated the safety and tolerability of Enoxacin and included the following safety assessments: adverse events (AEs), including AEs related to the drug, and serious AEs, i.e. AEs that affect patient’s safety and require medical intervention. Adverse events (AEs) were coded to preferred terms from the MedDRA library (version 23.0). Additional safety assessments included physical examination; body weight; 12-lead electrocardiogram (ECG) parameters; vital signs; laboratory safety assessments; and FVC

predicted percentage. The tolerability of Enoxacin was determined based on rates of AEs and the discontinuation of the study drug due to drug-related AEs.

Secondary outcomes included Amyotrophic Lateral Sclerosis Functional Rating Scale-Revised (ALSFRS-R) score at baseline and at the end of the follow-up period on day 30 and pharmacokinetic analysis of Enoxacin in plasma on days 1, 7, 14, 21 and 30 and of Riluzole on days 1 and 30. Additional secondary outcomes were unbiased analysis of miRNA levels and measurement of neurofilament light chain (NfL) levels in the plasma on days 1, 7, 14, 21 and 30 and in the CSF on days 1 and 28. An illustration of the study design and its endpoints is seen in Figure 2.

Biofluid collection

Phlebotomies were performed before Enoxacin morning dosing on days 1, 7 (+/- two days), 14 (+/- two days), 21 (+/- two days) and 30. After blood withdrawal, cells were pelleted by centrifugation at 2000 RPM for 10 minutes at 4°C. The plasma was transferred to a separate tube and stored at -80^{o}C. Cerebrospinal fluid (CSF) was collected by lumbar puncture (LP) before dosing on day 1, and two hours (+/-one hour) post dosing on day 28. CSF samples were centrifuged at 2000 RPM for 10 minutes at 4°C to pellet cells. LP was performed only for participants who specifically consented to this procedure.

Pharmacokinetic analysis

Trough plasma concentrations of Enoxacin (ng/ml) were measured before administration of the morning dose on days 1 (before treatment onset), 7, 14, 21, and 30 to determine steady-state levels. Plasma concentrations were also measured 1, 2, 4, 6, 8, and 24 hours after dosing on days 1 and 30 to determine C_{max} (maximal concentration) and t_{max} (time to reach maximal concentration) after a single dose of Enoxacin. Enoxacin concentrations were measured by liquid chromatography with tandem mass spectrometry (LC-MS/MS) at SGS Life Science Services (Saint-Benoît, France). Plasma concentrations of Riluzole (ng/ml) were measured 2, 4, 6 and 8 hours after Enoxacin dosing on days 1 and 30 to determine potential inhibitory effect of Enoxacin on Riluzole metabolism, as reported previously(62). Riluzole was measured by Protein-precipitation extraction / HPLC with MS/MS at Aliri Bioanalysis (Salt Lake City, Utah).

Biomarker assays

miRNA profiling. Total RNA was extracted from 0.5-1 ml of plasma or CSF using the miRNeasy micro kit (Qiagen, Hilden, Germany) by an experimenter blinded to the identity of samples. Repeated samples from the same individuals were processed in the same batch to avoid confounding effects of batch-to-batch variation on differences between repeated samples. Small RNA-seq libraries were prepared from 5µl total RNA using the QIAseq miRNA UDI Library Kit and QIAseq miRNA 96 Index Kit IL UDI-B (Qiagen) in a blinded fashion, keeping the same batches as library preparation. 3' and 5' adapter ligation was followed by reverse transcription. Precise linear quantification of miRNA was achieved by 12-nucleotide long unique molecular identifiers (UMIs) within the reverse transcription primers(63). cDNA libraries were amplified by 22 cycles (plasma) or 23 cycles (CSF) of PCR, with two unique dual indices (UDIs) of 10 nucleotides, followed by on-bead size selection and cleaning. Library concentration was determined with a Qubit fluorometer (dsDNA high sensitivity assay kit; Thermo Fisher Scientific, Waltham, MA) and library size with Tapestation D1000 (Agilent). Libraries with different indices were multiplexed and sequenced on Novaseq 6000 S1 flow cell (Illumina), with 72-bp single read and 10-bp read for index 1 and index 2. Fastq files were de-multiplexed and human miRNAs were mapped using miRBase(64) reference and the RNA-seq Analysis & Biomarker Discovery Portal (GeneGlobe, Qiagen).

Neurofilament analysis. NFL concentrations were measured in duplicates by a single molecule array (Simoa, Quanterix, Boston, MA, USA), using a bead-conjugated immunocomplex and NF-light Advantage Kit for HD-1/HD-X adjusted for SR-X (Uman Diagnostics Umea, Sweden). The immunocomplex was applied to a multi-well array designed to enable imaging of every single bead. A calibration curve constructed using serially diluted bovine NFL standard (UmanDiagnostics) enabled precise quantification of the average number of enzymes per bead per sample of plasma or CSF (diluted 1:4 and 1:100, respectively). The experimenter was blinded to labels and analysis comprised a single batch of reagents.

Statistical analysis

After alignment of sequencing reads to the human genome, only miRNAs with UMI counts >50 in at least 50% of plasma samples, or an average UMI count >20 across all samples in the CSF were included in the analysis. To reduce subject-to-subject variability, counts were batch-

corrected using the ComBat function, whereby each subject is considered a batch, as in our previous works (59, 60, 64). Batch-corrected counts were normalized to prevent sequencing biases in two manners: either by the levels of miR-451a, a dicer-independent miRNA (19), or by the DESeq2 algorithm which takes into account library size geometric mean (65), under the assumption that miRNA counts followed a negative binomial distribution. Total miRNA abundance was calculated by summing the abundances of all miRNAs.

Principal Component Analysis (PCA) was employed to reduce dataset dimensionality and to identify data patterns that correspond to the largest variances. Data were standardized to have a mean of zero and a standard deviation of one, ensuring that all variables contributed equally to the analysis and then eigenvalues and eigenvectors of the covariance matrix were calculated to determine the principal components. A transformation into a new coordinate system facilitated the visualization of only the two principal components with the largest variances being presented.

K-mean clustering was performed using R. Multiple miRNA expression was partitioned into predefined distinct non-overlapping clusters by minimizing the sum of distances between the data points and their respective cluster centroids. Data points consisted of each miRNA's mean abundance and fold change post-treatment vs baseline. Data were first normalized to prevent scale dependencies that could bias the distance calculations. Based on preliminary analysis data were divided into k=2 distinct clusters and a specific objective of our study aimed at understanding bifurcation in the data patterns.

Plasma NfL levels following treatment were analyzed with one-way repeated measures ANOVA. Plasma abundance of multiple miRNA species following treatment was analyzed by repeated measures two-way ANOVA wherein time point was included as a repeated factor and miRNA species as an additional factor. Pairwise comparisons were performed between post-treatment points (days 7, 14, 21 and 30) and baseline.

Comparison of plasma abundance of multiple miRNAs averaged over days 7, 14, 21 and 30 to baseline abundance, as well as of CSF abundance of multiple miRNAs post-treatment to baseline, was performed with paired t-tests for the different miRNA species, followed by correction to multiple hypotheses.

Post-treatment plasma total miRNA abundance was analyzed with a non-parametric Friedman

test, followed by pairwise time point comparisons (post-treatment vs. baseline). The significance of averaged plasma total miRNA abundance (days 7, 14, 21 and 30 averaged), as well as CSF total miRNA abundance and NfL (post-treatment vs. baseline), were determined with paired t-test.

In the case of multiple hypotheses testing (i.e. multiple time points tested vs baseline or multiple miRNAs tested between time points), p-values were corrected according to Benjamini and Hochberg (66), or the two-stage linear step-up procedure of Benjamini, Krieger, and Yekutieli (67). The false discovery rate (FDR) was set at 0.1. Statistical analyses were performed with R (version 4.2.0, R Foundation for Statistical Computing, Vienna, Austria) or GraphPad Prism version 10.2.3. (GraphPad Software, Boston, Massachusetts USA). Graphs were generated using Graphpad prism.

Study protocol and statistical analysis plan

The study protocol and statistical analysis plan are available in eSAP 1. Statistical analysis plan is included in section 6, page 62 of the study protocol. Due to the smaller number of patients recruited to the study than planned, some changes to the statistical analyses were made with respect to the original plan.

Results

Safety and tolerability of Enoxacin in people living with ALS

A total of 13 people living with ALS were screened for the study, of whom 8 passed screening (Figure 1). Recruitment occurred between April 2021 and March 2023, and the last patient follow up was in April 2023. Participants' baseline characteristics are presented in Table 1. While all participants experienced adverse events (AEs; Table 2), most of the AEs reported were mild (36/52 events, 69%). The remaining AEs were moderate (13/52, 25%) or severe (3/52, 6%). There were no life-threatening, or serious, events (0/52). The three severe AEs were as follows: deep vein thrombosis in one patient (dosed at 200mg x 2/day), was probably not related to Enoxacin and was resolved after increasing the dose of an anticoagulant, apixaban, which the patient has been taking regularly for at least six years. Nausea in another patient (dosed at 200mg x 2/day), was resolved after taking dimenhydrinate (Dramamine). Dizziness in a third patient (dosed at 400mg x 2/day), decreased in severity during the next visit without medical intervention.

One patient in the 600mg x 2/day dosing group experienced AEs (nausea and dizziness) that were assessed as related to Enoxacin. These were defined as mild or moderate (Table 2), were not life threatening, but were symptomatically severe enough to cause early discontinuation of Enoxacin before completion of the dosing period.

AEs related to Enoxacin did not cause an early drop-out in any other patient and all participants other than one completed the dosing period and did not miss any dose of Enoxacin. In addition, throughout the dosing period none of the patients presented significant abnormalities in ECG, vital signs (blood pressure and pulse rate), or blood tests. All the AEs seen were previously observed in the original development of Enoxacin for antimicrobial indications. In addition, although potential interaction of Enoxacin with Riluzole was suggested in vitro (62), none of the AEs were deemed related to a possible change in Riluzole levels. Therefore, we concluded that Enoxacin at 200mg x 2/day and 400mg x2/day was generally safe and well-tolerated, encouraging in-depth analysis of data associated with these two doses (n=3 per dose).

Pharmacokinetic study of Enoxacin and Riluzole

Molecular measurements were pooled from the two dose groups analyzed, due to the small number of observations in each dose (n=3). Average Enoxacin plasma concentrations on days 7,14, 21, and 30 before the morning dose were 628±286, 563±250, 548±288 and 685±296 ng/ml, respectively (Supplementary table 1). Average C_{max} reached within two hours of administration were 1324±477 and 1752±475 ng/ml on days 1 and 30, respectively. Enoxacin trough concentrations were rather constant from day 7 until the end of drug dosing on day 30. Therefore, Enoxacin levels were at a steady state at the time points in which pharmacodynamic markers were measured.

Riluzole concentrations were measured at 2h, 4h, 6h and 8h after Enoxacin administration on days 1 and 30. Higher Riluzole concentrations on day 30 (Supplementary table 2), suggests an Enoxacin-Riluzole interaction, in agreement with reported in vitro effects(62). However, measured Riluzole levels did not exceed the C_{max} reported to be safe, given a dose of 50mg BID twice daily(68, 69). This suggests Riluzole levels are within the safe range, in agreement with lack of adverse events related to Riluzole.

Enoxacin elevates miRNA levels in the plasma

Enoxacin is an agonist of the Dicer complex(21, 23, 25) and is expected to upregulate miRNA biogenesis in tissues(14). To address the hypothesis that the impact of Enoxacin on miRNA can be detected in biofluids, we have profiled cell-free miRNAs in an unbiased manner by next-generation miRNA sequencing. We hypothesized that Enoxacin would elevate the levels of many miRNAs and that accordingly miRNA could serve as a pharmacodynamic (PD) marker of target engagement.

Plasma samples were collected by phlebotomy at baseline, before treatment initiation, and on days 7, 14, 21, and 30 before the morning dose. Small RNA libraries were prepared and sequenced on the Illumina NovaSeq platform with a 72-bp single read, followed by mapping of gained sequences into the human genome. As many as 2632 individual miRNA species were aligned to the human genome (GRCh37/hg19) across all samples. We included in the downstream analysis only miRNAs with UMI counts >50 in at least 50% of plasma samples (N=92 miRNAs). The repeated sampling from subjects allowed us to estimate the mean shift in

read counts associated with each subject. We adjusted the original counts using this estimated parameter, to reduce the confounding effect of subject-to-subject variability. Adjusted counts in each sample were then normalized to the sample levels of miR-451a, a Dicer-independent miRNA (19), and analyzed for the difference in abundance between post-treatment time points and baseline.

Between 36% and 47% of the 92 miRNAs included in the analysis increased significantly (33/92, 36/92, 43/92, 33/92 on days 7, 14, 21, and 30 respectively, Figure 3A-D). 59 miRNAs, which are 64% of all miRNAs, increased significantly when miRNA abundance was averaged across all post-treatment time points (Figure 3E). In order to reduce the dimensionality of the dataset which is composed of multiple miRNAs, we ran principal component analysis (PCA) on the levels of all miRNAs averaged on days 7, 14, 21 and 30 and their baseline levels in individual samples. Baseline samples and post-treatment samples were well-separated (Figure 3F). However, the post-treatment samples are more clustered than the baseline samples, suggesting that Enoxacin reduces variability in miRNA levels between samples, which may result from reaching a maximal effect on dicer activity.

Notable miRNAs that increased are the miR-320 family members (miR-320a, miR-320b, miR-320c, and miR-320d), the muscle-enriched miR-206 and miR-378a, miR-423 which increased longitudinally in ALS patients in our previous work(59) and the blood enriched miR-486-5p. Importantly, a few miRNAs decreased but to a small extent and in a non-significant manner, demonstrating a preference for Enoxacin toward increasing miRNA levels as previously reported(21, 23).

When miRNA levels were normalized by the DESeq2 method(65), 15 miRNAs increased significantly on day 7, 14 on day 14, 18 on day 21 and 15 on day 30. In contrast, miR-451a decreased significantly at all time points, in agreement with the previous report on the effects of Dicer enhancement(20) (Supp. figure 1A-D). When miRNA abundance was averaged across post-treatment time points, out of the total increased miRNAs (Log 2-fold change > 0), 19 were statistically significant (19/46, 41.3%), in comparison to the five miRNAs that decreased significantly out of the total decreased ones (Log 2-fold change < 0, 5/47, 10.6%) (Supp. Figure 1E). This difference in proportion was statistically significant (p=0.0007, chi-square test), supporting a preference toward increasing miRNA levels. Notably, miR-320 family members

and miR-423 were found to increase significantly at all time points regardless of the normalization method, suggesting a robust effect of Enoxacin on these miRNAs. We ran PCA on miRNA levels normalized by DESeq2 as we did for miRNA levels normalized to miR-451a (Figure 3F) and found a separation between baseline and post-treatment samples (Supp. Figure 1F), which supports a strong and positive effect of Enoxacin on miRNA levels.

We next grouped miRNAs into distinct groups, based on similar mean abundance and fold change. This step simplifies data interpretation and highlights miRNAs that consistently behave similarly under the effect of Enoxacin, suggesting they might have related biological functions or regulatory mechanisms. Thus, the 92 miRNAs are clustered for each time point and for the average of all time points via K-means clustering. miR-16, miR-423, and miR-486-5p clustered together, in combination with let-7b/a (Figure 4) and may serve as potential biomarkers set for the molecular response to Enoxacin.

We next compared the total abundance of miRNAs on days 7, 14, 21, and 30 and at all post-treatment time points averaged, to baseline. Total miRNA abundance was calculated by summing the abundance of all individual miRNAs normalized to miR-451a abundance. There was an overall increase in total miRNA abundance when each post-treatment time point was compared to the baseline (Friedman test: $p<0.01$, Figure 5A). The highest increases in total miRNA abundances were observed on days 14 and 21: 3.4-fold and 3.1-fold, respectively, from 170±45 UMIs at baseline to 583±381 UMIs on day 14, and 526±226 UMIs on day 21 (q value = 0.007 and 0.004, respectively, after multiple hypothesis correction). In addition, total miRNA abundance at all post-treatment time points averaged was 2.5-fold higher than baseline (422±17.5 UMIs vs 170±45 UMIs, paired t-test: $p<0.0001$, Figure 5B).

A similar analysis was performed when total miRNA abundance was normalized to size factor by the DESeq2 method (Supp. Figure 2). Total miRNA abundance increased on day 14 compared to baseline in a significant manner (Supp. Figure 2A, paired t-test uncorrected p-value: 0.045) and approached significance on day 21 (uncorrected p-value=0.052). Furthermore, total miRNA abundance at all post-treatment time points averaged was higher than baseline (paired t-test: $p=0.042$, Supp. Figure 2B).

Taken together, Enoxacin elevates miRNA levels in plasma at all time points compared to baseline with two different normalization methods, with a more robust effect when miRNA

levels are normalized to the opposite effect of reducing miR-451a levels. The data suggest target engagement of Enoxacin with Dicer and corroborates previous works measuring miRNA in animal tissues.

Enoxacin elevates miRNA levels in the CSF

Having found that Enoxacin elevates miRNAs in the plasma, we next compared miRNA abundance in the CSF between post-treatment and baseline samples collected from patients who specifically consented to this procedure (n=4). As opposed to plasma, CSF reflects the cerebral microenvironment and thus can be a better approximation of the Enoxacin effect in the brain. We first compared the levels of miR-451a to confirm the inhibitory effect that we found in plasma. Similar to plasma, miR-451a significantly decreased by 40%, from 14.8±1.8 UMIs at baseline to 8.85±1.6 UMIs post-treatment (Figure 6A, paired t-test: p=0.04). We then normalized all miRNA levels to miR-451a, as was done in plasma. Total miRNA abundance in the CSF, after normalization to miR-451a, significantly increased by 70%, from 731±37 UMIs at baseline to 1259±86 UMIs post-treatment (Figure 6B, paired t-test: p=0.018).

We further compared the levels of individual miRNAs post-treatment to their baseline levels, focusing only on 30 miRNAs that exhibited significant increase at all time points in plasma (Supp. table 3), to reduce the number of corrected hypotheses. Five of these 30 miRNAs - miR-139, miR-210, miR-339, miR-4508 and miR-4732 - did not pass the threshold of abundance in the CSF and were therefore not included in the analysis. Eight miRNAs were found to be significantly elevated in the CSF, after correction for multiple hypotheses: let-7c, miR-2110, miR-378a, miR-423 and the four members of the miR-320 family: miR-320a, miR-320b, miR-320c and miR-320d (Figure 6C). Of all miRNAs, miR-378a exhibited the highest increase compared to baseline: 3.4-fold. Notably, miR-320 family members and miR-423 were also elevated in the plasma, suggesting that they are the most affected by Enoxacin.

An additional biomarker which we measured in the circulation is NfL, which was a molecular endpoint in a recent clinical trial(2). As was expected by the short period of therapy, NfL levels in the plasma and the CSF did not reveal any significant differences at any time point post-treatment compared to baseline (Supp. Figure 3).

Pharmacokinetic-pharmacodynamic relationship

Once we established the effect of Enoxacin on miRNA levels in both the plasma and CSF, we wished to study the pharmacokinetics-pharmacodynamic (PK-PD) relationship, i.e. association between plasma through Enoxacin concentrations and matching fold-change values of miRNAs compared to baseline. We analyzed the correlation between Enoxacin concentrations and fold-change values on day 14, where the maximal effect of Enoxacin on total miRNA abundance was observed (Figure 5). One data point was omitted due to a technical failure in measuring Enoxacin. Figure 7 presents the Pearson correlation of 13 miRNAs, which were significantly elevated by Enoxacin on day 14 (Figure 3B) and were in addition significantly correlated with Enoxacin concentrations after testing correlations for all miRNAs and correcting for multiple hypotheses (FDR<0.1). miR-139, miR-185, miR-320a, miR-320d, miR-339, miR-629, and miR-652 had a correlation > 0.95, which, together with a high fold- change on day 14 (>2.5, Figure 3B), suggests a strong effect of Enoxacin on these miRNAs. The fold-change of miR-423 which forms a cluster with miR-486 and miR-16 (Figure 4) exhibited a correlation coefficient of 0.93 with Enoxacin (Figure 7J), further suggesting it may be a strong candidate biomarker for Enoxacin.

Discussion

While the safety profile of Enoxacin is known and this drug has been in clinical use for many years, this trial examined for the first time the safety and tolerability of Enoxacin in patients with ALS in three doses of 200mg x 2/day, 400mg x 2/day and 600mg x2/day over a 30 days period of oral administration. At 600mg x2/day one patient dropped out before study completion, due to AEs that were deemed to be related to the drug. WE conclude that Enoxacin is generally safe in patients with ALS and is well-tolerated at doses of 200mg x 2/day and 400mg x 2/day.

We focused our study on measuring miRNAs as biomarkers and molecular endpoints for the effects of Enoxacin. Because of the known effect of Enoxacin on DICER and its substrate, miRNAs, we profiled miRNAs as pharmacodynamic and target engagement biomarkers. Most of the miRNAs were increased as a result of Enoxacin treatment in both plasma and CSF, supporting the engagement of Enoxacin with its target. The extent of the effect of Enoxacin on miRNAs. i.e. the increase in their levels was correlated with the concentration of Enoxacin in the plasma, which further supports target engagement.

A main question of our study was whether Enoxacin could have an effect in the CSF, a potential reflection of the central nervous system as the target tissue. Previous works show that the ratio of CSF to plasma levels is 33.3% in dogs(70), and 20% in rats(71, 72), suggesting substantial penetration of Enoxacin into the CSF from the blood. One study found a ratio of 29% in the CSF and 10% in the brain of rats(73). In agreement with these studies, we observed an effect of Enoxacin on miRNA levels in the CSF, and three of the miRNAs that were increased in the CSF - let-7c, miR-16 and miR-320a - are abundant in both the human brain and spinal cord (>1000 copies)(74). Together, the findings suggest that Enoxacin can affect miRNA biogenesis within the central nervous system when administered orally.

Some of the miRNAs that were increased by Enoxacin treatment were reported to be neuroprotective, in the context of ALS or brain injuries. For instance, miR-139 was downregulated in postmortem motor neurons of ALS patients by 8-fold(15), and in ALS iPSC-derived motor neurons, leading to upregulation of the Wnt/β-catenin pathway which is a driver of motor neuron degeneration(75). Thus, restoring miR-139 levels in ALS may be beneficial to motor neurons by regulating the Wnt/β-catenin pathway. Other miRNA that were increased by

Enoxacin were miR-130a, which displays neuroprotective activity after cerebral ischemia upstream of the PTEN/PI3K/AKT pathway(76-78), Let-7c, miR-378a, miR-486 and miR-93 that were reported to regulate microglial activation, suppress neuroinflammation and inhibit neuronal apoptosis in cerebral ischemia and traumatic brain injury(79-83) and miR-30e that regulated neuroinflammation in a Parkinson's disease model(84).

Some of the miRNAs that were increased by Enoxacin were reduced in biofluids and tissues from ALS patients or ALS mouse models, suggesting that Enoxacin recovers the expression of these miRNAs. For example, miR-378a levels are reduced in CSF from ALS patients (58) and were increased in the CSF following Enoxacin. miR-320 levels are reduced in the serum or CSF of patients with ALS(47) or FTD (85, 86) and in the spinal cord and brainstem of SOD1 G93A mice (87) and are increased in response to Enoxacin therapy.

The recent approval of Tofersen as a therapy for ALS by the FDA, based on its ability to lower blood levels of neurofilament light (NfL)(88) highlights the importance of biomarkers as an endpoint for clinical trials. The fact that Enoxacin did not affect NfL levels in our trial suggests that elevation of miRNA levels for only one month is insufficient to affect axonal integrity, but an effect could be potentially observed with a longer duration of therapy.

Limitations

The small cohort size hindered determining whether the effect of Enoxacin on miRNAs was dose-dependent. Furthermore, the study did not explore efficacy as an endpoint, due to the short therapy time and small number of patients.

In summary, Enoxacin presents a promising therapeutic option for ALS with an established safety profile, robust mechanistic data, and evidence for target engagement in both human patient plasma and CSF. The ready-to-use pharmacodynamic biomarker package enhances its appeal as a testable compelling addition to the ALS treatment landscape.

Data availability

Data is available upon reasonable request from the author.

Acknowledgments

EH is the Mondry Family Professorial Chair and Head of the Nella and Leon Benoziyo Centre for Neurological Diseases and of the Andi and Larry Wolfe Centre for Neuroimmunology and Neuromodulation. We thank Orla Hardiman (Trinity College Dublin), Dame Pamela Shaw (University of Sheffield), and Leonard van den Berg (University Medical Center Utrecht) for their advice on the study design. We are grateful to Susan Stern, National Executive Director and CEO of Weizmann Canada, and Prof. Erik Storkebaum (Radboud University, Nijmegen) for their involvement. Enoxacin was an in-kind gift from the late Barry Sherman, Alexandra Krawczyk, the Honey & Barry Sherman Legacy Foundation and Apotex Inc., Toronto, Canada. We thank Drs. Brigitte Happ, Kostas Kaloulis, Sonia Poli and Dawn Toronto for their consultation on drug development and regulatory affairs. We thank Yahel Cohen and Dr. Nancy S Yacovzda (WIS) for advice and for comments on the manuscript.

Funding

This study was funded by ALS Association clinical trial award (program: 'Repurposing Enoxacin therapy for patients with ALS' 22-CTA-614), ALS Canada-Brain Canada Discovery grant (program: 'Advanced Pharmacokinetics and Pharmacodynamics for phase Ib/IIa trial of repurposed Enoxacin therapy for patients with ALS'), ERA-Net for Research Programs on Rare Diseases (eRARE FP7) via the Israel Ministry of Health and Muscular Dystrophy Canada, Canadian Institutes of Health Research (CIHR) and Fonds de recherche du Québec - Santé (FRQS). IM was supported by Teva Pharmaceutical Industries as part of the Israeli National Network of Excellence in Neuroscience (fellowship no. 117941).

Research at the Hornstein lab is further funded by Andi and Larry Wolfe Centre for Neuroimmunology and Neuromodulation, the Binational Science Foundation (BSF); Association Française Contre les Myopathies (AFM) grants 24882, 28680; Muscular Dystrophy Association (MDA) grant 1280000; Target ALS; Israel Science Foundation (ISF 3497/21, 424/22); ALS Canada; Minna-James-Heineman Stiftung through Minerva, Minerva Foundation, with funding from the Federal German Ministry for Education and Research; Robert Packard Center for ALS Research at Johns Hopkins; McGill University; EU - ERA-Net; Radala Foundation for ALS Research; Additional support generously provided by the Kekst Family Institute for Medical Genetics. Weizmann SABRA - Yeda-Sela - WRC Program, the

Estate of Emile Mimran, and The Maurice and Vivienne Wohl Biology Endowment. Nella and Leon Benoziyo Center for Neurological Diseases. Goldhirsh-Yellin Foundation. Dr. Sydney Brenner and friends. Weizmann - Center for Research on Neurodegeneration. Redhill Foundation – Sam and Jean Rothberg Charitable Trust Dr. Dvora and Haim Teitelbaum Endowment Fund.

The funders were not involved in study design; collection, management, analysis and interpretation of data; or the decision to submit for publication.

Competing interests

The authors have no competing interests to report.

References

1. Tsai M-J, Hsu C-Y, Sheu C-C. Amyotrophic Lateral Sclerosis. N Engl J Med. 2017;377(16):1602.
2. Miller TM, Cudkowicz ME, Genge A, Shaw PJ, Sobue G, Bucelli RC, et al. Trial of Antisense Oligonucleotide Tofersen for SOD1 ALS. N Engl J Med. 2022;387(12):1099-110.
3. Al-Chalabi A, van den Berg LH, Veldink J. Gene discovery in amyotrophic lateral sclerosis: implications for clinical management. Nat Rev Neurol. 2017;13(2):96-104.
4. Haramati S, Chapnik E, Sztainberg Y, Eilam R, Zwang R, Gershoni N, et al. miRNA malfunction causes spinal motor neuron disease. Proc Natl Acad Sci U S A. 2010;107(29):13111-6.
5. Lagier-Tourenne C, Cleveland DW. Rethinking ALS: the FUS about TDP-43. Cell. 2009;136(6):1001-4.
6. Lagier-Tourenne C, Polymenidou M, Cleveland DW. TDP-43 and FUS/TLS: emerging roles in RNA processing and neurodegeneration. Hum Mol Genet. 2010;19(R1):R46-64.
7. Lemmens R, Moore MJ, Al-Chalabi A, Brown RH, Jr., Robberecht W. RNA metabolism and the pathogenesis of motor neuron diseases. Trends Neurosci. 2010;33(5):249-58.
8. Strong MJ. The evidence for altered RNA metabolism in amyotrophic lateral sclerosis (ALS). J Neurol Sci. 2010;288(1-2):1-12.
9. Irwin KE, Jasin P, Braunstein KE, Sinha IR, Garret MA, Bowden KD, et al. A fluid biomarker reveals loss of TDP-43 splicing repression in presymptomatic ALS-FTD. Nat Med. 2024;30(2):382-93.
10. Keuss MJ, Harley P, Ryadnov E, Jackson RE, Zanovello M, Wilkins OG, et al. Loss of TDP-43 induces synaptic dysfunction that is rescued by UNC13A splice-switching ASOs. bioRxiv. 2024.
11. Costantino I, Meng A, Ravits J. Alternatively spliced ELAVL3 cryptic exon 4a causes ELAVL3 downregulation in ALS TDP-43 proteinopathy. Acta Neuropathol. 2024;147(1):93.
12. Cao MC, Ryan B, Wu J, Curtis MA, Faull RLM, Dragunow M, et al. A panel of TDP-43-regulated splicing events verifies loss of TDP-43 function in amyotrophic lateral sclerosis brain tissue. Neurobiol Dis. 2023;185:106245.
13. Campos-Melo D, Droppelmann CA, He Z, Volkening K, Strong MJ. Altered microRNA expression profile in Amyotrophic Lateral Sclerosis: a role in the regulation of NFL mRNA levels. Mol Brain. 2013;6:26.
14. Emde A, Eitan C, Liou L-L, Libby RT, Rivkin N, Magen I, et al. Dysregulated miRNA biogenesis downstream of cellular stress and ALS-causing mutations: a new mechanism for ALS. EMBO J. 2015;34(21):2633-51.
15. Figueroa-Romero C, Hur J, Lunn JS, Paez-Colasante X, Bender DE, Yung R, et al. Expression of microRNAs in human post-mortem amyotrophic lateral sclerosis spinal cords provides insight into disease mechanisms. Mol Cell Neurosci. 2016;71:34-45.
16. Reichenstein I, Eitan C, Diaz-Garcia S, Haim G, Magen I, Siany A, et al. Human genetics and neuropathology suggest a link between miR-218 and amyotrophic lateral sclerosis pathophysiology. Sci Transl Med. 2019;11(523).
17. Kawahara Y, Mieda-Sato A. TDP-43 promotes microRNA biogenesis as a component of the Drosha and Dicer complexes. Proc Natl Acad Sci U S A. 2012;109(9):3347-52.
18. Bernstein E, Caudy AA, Hammond SM, Hannon GJ. Role for a bidentate ribonuclease in the initiation step of RNA interference. Nature. 2001;409(6818):363-6.
19. Yang J-S, Maurin T, Robine N, Rasmussen KD, Jeffrey KL, Chandwani R, et al.

Conserved vertebrate mir-451 provides a platform for Dicer-independent, Ago2-mediated microRNA biogenesis. Proc Natl Acad Sci U S A. 2010;107(34):15163-8.
20. Kretov DA, Walawalkar IA, Mora-Martin A, Shafik AM, Moxon S, Cifuentes D. Ago2-Dependent Processing Allows miR-451 to Evade the Global MicroRNA Turnover Elicited during Erythropoiesis. Mol Cell. 2020;78(2):317-28.e6.
21. Melo S, Villanueva A, Moutinho C, Davalos V, Spizzo R, Ivan C, et al. Small molecule enoxacin is a cancer-specific growth inhibitor that acts by enhancing TAR RNA-binding protein 2-mediated microRNA processing. Proc Natl Acad Sci U S A. 2011;108(11):4394-9.
22. Schaeffer AJ. The expanding role of fluoroquinolones. Am J Med. 2002;113 Suppl 1A:45S-54S.
23. Shan G, Li Y, Zhang J, Li W, Szulwach KE, Duan R, et al. A small molecule enhances RNA interference and promotes microRNA processing. Nat Biotechnol. 2008;26(8):933-40.
24. Smalheiser NR, Zhang H, Dwivedi Y. Enoxacin Elevates MicroRNA Levels in Rat Frontal Cortex and Prevents Learned Helplessness. Front Psychiatry. 2014;5:6.
25. Rizzuti M, Filosa G, Melzi V, Calandriello L, Dioni L, Bollati V, et al. MicroRNA expression analysis identifies a subset of downregulated miRNAs in ALS motor neuron progenitors. Sci Rep. 2018;8(1):10105.
26. Shelkovnikova TA, Kukharsky MS, An H, Dimasi P, Alexeeva S, Shabir O, et al. Protective paraspeckle hyper-assembly downstream of TDP-43 loss of function in amyotrophic lateral sclerosis. Mol Neurodegener. 2018;13(1):30.
27. Arakawa Y, Itoh S, Fukazawa Y, Ishiguchi H, Kohmoto J, Hironishi M, et al. Association between oxidative stress and microRNA expression pattern of ALS patients in the high-incidence area of the Kii Peninsula. Brain Res. 2020;1746:147035.
28. Banack SA, Dunlop RA, Cox PA. An miRNA fingerprint using neural-enriched extracellular vesicles from blood plasma: towards a biomarker for amyotrophic lateral sclerosis/motor neuron disease. Open Biol. 2020;10(6):200116.
29. Benigni M, Ricci C, Jones AR, Giannini F, Al-Chalabi A, Battistini S. Identification of miRNAs as Potential Biomarkers in Cerebrospinal Fluid from Amyotrophic Lateral Sclerosis Patients. Neuromolecular Med. 2016;18(4):551-60.
30. Cloutier F, Marrero A, O'Connell C, Morin P, Jr. MicroRNAs as potential circulating biomarkers for amyotrophic lateral sclerosis. J Mol Neurosci. 2015;56(1):102-12.
31. Daneshafrooz N, Joghataei MT, Mehdizadeh M, Alavi A, Barati M, Panahi B, et al. Identification of let-7f and miR-338 as plasma-based biomarkers for sporadic amyotrophic lateral sclerosis using meta-analysis and empirical validation. Sci Rep. 2022;12(1):1373.
32. de Andrade HMT, de Albuquerque M, Avansini SH, de S Rocha C, Dogini DB, Nucci A, et al. MicroRNAs-424 and 206 are potential prognostic markers in spinal onset amyotrophic lateral sclerosis. J Neurol Sci. 2016;368:19-24.
33. De Felice B, Annunziata A, Fiorentino G, Borra M, Biffali E, Coppola C, et al. miR-338-3p is over-expressed in blood, CFS, serum and spinal cord from sporadic amyotrophic lateral sclerosis patients. Neurogenetics. 2014;15(4):243-53.
34. De Luna N, Turon-Sans J, Cortes-Vicente E, Carrasco-Rozas A, Illán-Gala I, Dols-Icardo O, et al. Downregulation of miR-335-5P in Amyotrophic Lateral Sclerosis Can Contribute to Neuronal Mitochondrial Dysfunction and Apoptosis. Sci Rep. 2020;10(1):4308.
35. Dobrowolny G, Martone J, Lepore E, Casola I, Petrucci A, Inghilleri M, et al. A longitudinal study defined circulating microRNAs as reliable biomarkers for disease prognosis and progression in ALS human patients. Cell Death Discov. 2021;7(1):4.
36. Freischmidt A, Müller K, Zondler L, Weydt P, Mayer B, von Arnim CAF, et al. Serum microRNAs in sporadic amyotrophic lateral sclerosis. Neurobiol Aging. 2015;36(9):2660.e15-20.
37. Giagnorio E, Malacarne C, Cavalcante P, Scandiffio L, Cattaneo M, Pensato V, et al. MiR-146a in ALS: Contribution to Early Peripheral Nerve Degeneration and Relevance as Disease Biomarker. Int J Mol Sci. 2023;24(5).
38. Joilin G, Gray E, Thompson AG, Bobeva Y, Talbot K, Weishaupt J, et al. Identification of a potential non-coding RNA biomarker signature for amyotrophic lateral sclerosis. Brain Commun. 2020;2(1):fcaa053.

39. Joilin G, Leigh PN, Newbury SF, Hafezparast M. An Overview of MicroRNAs as Biomarkers of ALS. Front Neurol. 2019;10:186.
40. Katsu M, Hama Y, Utsumi J, Takashina K, Yasumatsu H, Mori F, et al. MicroRNA expression profiles of neuron-derived extracellular vesicles in plasma from patients with amyotrophic lateral sclerosis. Neurosci Lett. 2019;708:134176.
41. Liguori M, Nuzziello N, Introna A, Consiglio A, Licciulli F, D'Errico E, et al. Dysregulation of MicroRNAs and Target Genes Networks in Peripheral Blood of Patients With Sporadic Amyotrophic Lateral Sclerosis. Front Mol Neurosci. 2018;11:288.
42. Lo T-W, Figueroa-Romero C, Hur J, Pacut C, Stoll E, Spring C, et al. Extracellular Vesicles in Serum and Central Nervous System Tissues Contain microRNA Signatures in Sporadic Amyotrophic Lateral Sclerosis. Front Mol Neurosci. 2021;14:739016.
43. Malacarne C, Galbiati M, Giagnorio E, Cavalcante P, Salerno F, Andreetta F, et al. Dysregulation of Muscle-Specific MicroRNAs as Common Pathogenic Feature Associated with Muscle Atrophy in ALS, SMA and SBMA: Evidence from Animal Models and Human Patients. Int J Mol Sci. 2021;22(11).
44. Matamala JM, Arias-Carrasco R, Sanchez C, Uhrig M, Bargsted L, Matus S, et al. Genome-wide circulating microRNA expression profiling reveals potential biomarkers for amyotrophic lateral sclerosis. Neurobiol Aging. 2018;64:123-38.
45. Panio A, Cava C, D'Antona S, Bertoli G, Porro D. Diagnostic Circulating miRNAs in Sporadic Amyotrophic Lateral Sclerosis. Front Med. 2022;9:861960.
46. Pregnolato F, Cova L, Doretti A, Bardelli D, Silani V, Bossolasco P. Exosome microRNAs in Amyotrophic Lateral Sclerosis: A Pilot Study. Biomolecules. 2021;11(8).
47. Raheja R, Regev K, Healy BC, Mazzola MA, Beynon V, Von Glehn F, et al. Correlating serum microrna and clinical parameters in amyotrophic lateral sclerosis. Muscle Nerve. 2018;58(2):261-9.
48. Ravnik-Glavač M, Glavač D. Circulating RNAs as Potential Biomarkers in Amyotrophic Lateral Sclerosis. Int J Mol Sci. 2020;21(5).
49. Ricci C, Marzocchi C, Battistini S. MicroRNAs as Biomarkers in Amyotrophic Lateral Sclerosis. Cells. 2018;7(11).
50. Saucier D, Wajnberg G, Roy J, Beauregard A-P, Chacko S, Crapoulet N, et al. Identification of a circulating miRNA signature in extracellular vesicles collected from amyotrophic lateral sclerosis patients. Brain Res. 2019;1708:100-8.
51. Sheinerman KS, Toledo JB, Tsivinsky VG, Irwin D, Grossman M, Weintraub D, et al. Circulating brain-enriched microRNAs as novel biomarkers for detection and differentiation of neurodegenerative diseases. Alzheimers Res Ther. 2017;9(1):89.
52. Soliman R, Mousa NO, Rashed HR, Moustafa RR, Hamdi N, Osman A, et al. Assessment of diagnostic potential of some circulating microRNAs in Amyotrophic Lateral Sclerosis Patients, an Egyptian study. Clin Neurol Neurosurg. 2021;208:106883.
53. Sproviero D, Gagliardi S, Zucca S, Arigoni M, Giannini M, Garofalo M, et al. Different miRNA Profiles in Plasma Derived Small and Large Extracellular Vesicles from Patients with Neurodegenerative Diseases. Int J Mol Sci. 2021;22(5).
54. Takahashi I, Hama Y, Matsushima M, Hirotani M, Kano T, Hohzen H, et al. Identification of plasma microRNAs as a biomarker of sporadic Amyotrophic Lateral Sclerosis. Mol Brain. 2015;8(1):67.
55. Tasca E, Pegoraro V, Merico A, Angelini C. Circulating microRNAs as biomarkers of muscle differentiation and atrophy in ALS. Clin Neuropathol. 2016;35(1):22-30.
56. Toivonen JM, Manzano R, Oliván S, Zaragoza P, García-Redondo A, Osta R. MicroRNA-206: a potential circulating biomarker candidate for amyotrophic lateral sclerosis. PLoS One. 2014;9(2):e89065.
57. Waller R, Goodall EF, Milo M, Cooper-Knock J, Da Costa M, Hobson E, et al. Serum miRNAs miR-206, 143-3p and 374b-5p as potential biomarkers for amyotrophic lateral sclerosis (ALS). Neurobiol Aging. 2017;55:123-31.
58. Waller R, Wyles M, Heath PR, Kazoka M, Wollff H, Shaw PJ, et al. Small RNA Sequencing of Sporadic Amyotrophic Lateral Sclerosis Cerebrospinal Fluid Reveals Differentially Expressed miRNAs Related to Neural and Glial Activity. Front Neurosci. 2017;11:731.
59. Magen I, Yacovzada NS, Yanowski E, Coenen-Stass A, Grosskreutz J, Lu C-H, et al. Circulating miR-181 is a prognostic biomarker for amyotrophic lateral sclerosis. Nat

Neurosci. 2021;24(11):1534-41.
60. Magen I, Aharoni S, Yacovzada NS, Tokatly Latzer I, Alves CRR, Sagi L, et al. Muscle microRNAs in the cerebrospinal fluid predict clinical response to nusinersen therapy in type II and type III spinal muscular atrophy patients. Eur J Neurol. 2022;29(8):2420-30.
61. Magen I, Yacovzada N-S, Warren JD, Heller C, Swift I, Bobeva Y, et al. microRNA-based predictor for diagnosis of frontotemporal dementia. Neuropathol Appl Neurobiol. 2023;49(4):e12916.
62. Sanderink GJ, Bournique B, Stevens J, Petry M, Martinet M. Involvement of human CYP1A isoenzymes in the metabolism and drug interactions of riluzole in vitro. J Pharmacol Exp Ther. 1997;282(3):1465-72.
63. Coenen-Stass AML, Magen I, Brooks T, Ben-Dov IZ, Greensmith L, Hornstein E, et al. Evaluation of methodologies for microRNA biomarker detection by next generation sequencing. RNA Biol. 2018;15(8):1133-45.
64. Kozomara A, Griffiths-Jones S. miRBase: annotating high confidence microRNAs using deep sequencing data. Nucleic Acids Res. 2014;42(Database issue):D68-73.
65. Love MI, Huber W, Anders S. Moderated estimation of fold change and dispersion for RNA-seq data with DESeq2. Genome Biol. 2014;15(12):550.
66. Benjamini Y, Drai D, Elmer G, Kafkafi N, Golani I. Controlling the false discovery rate in behavior genetics research. Behav Brain Res. 2001;125(1-2):279-84.
67. Benjamini Y, Krieger AM, Yekutieli D. Adaptive linear step-up procedures that control the false discovery rate. Biometrika. 2006;93(3):491-507.
68. Le Liboux A, Lefebvre P, Le Roux Y, Truffinet P, Aubeneau M, Kirkesseli S, et al. Single- and multiple-dose pharmacokinetics of riluzole in white subjects. J Clin Pharmacol. 1997;37(9):820-7.
69. Wymer J, Apple S, Harrison A, Hill BA. Pharmacokinetics, Bioavailability, and Swallowing Safety With Riluzole Oral Film. Clin Pharmacol Drug Dev. 2023;12(1):57-64.
70. Tran Van T, Armengaud A, Davet B. Diffusion of enoxacin into the cerebrospinal fluid in dogs with healthy meninges and with experimental meningitis. J Antimicrob Chemother. 1984;14 Suppl C:57-62.
71. Delon A, Bouquet S, Huguet F, Brunet V, Courtois P, Couet W. Pharmacokinetic-pharmacodynamic contributions to the convulsant activity of fluoroquinolones in rats. Antimicrob Agents Chemother. 1999;43(6):1511-5.
72. Marchand S, Pariat C, Boulanger A, Bouquet S, Couet W. A pharmacokinetic/pharmacodynamic approach to show that not all fluoroquinolones exhibit similar sensitivity toward the proconvulsant effect of biphenyl acetic acid in rats. J Antimicrob Chemother. 2001;48(6):813-20.
73. Kawakami J, Ohashi K, Yamamoto K, Sawada Y, Iga T. Effect of acute renal failure on neurotoxicity of enoxacin in rats. Biol Pharm Bull. 1997;20(8):931-4.
74. Keller A, Gröger L, Tschernig T, Solomon J, Laham O, Schaum N, et al. miRNATissueAtlas2: an update to the human miRNA tissue atlas. Nucleic Acids Res. 2022;50(D1):D211-D21.
75. Hawkins S, Namboori SC, Tariq A, Blaker C, Flaxman C, Dey NS, et al. Upregulation of β-catenin due to loss of miR-139 contributes to motor neuron death in amyotrophic lateral sclerosis. Stem Cell Reports. 2022;17(7):1650-65.
76. Wang Y, Gu J, Hu L, Kong L, Wang T, Di M, et al. miR-130a alleviates neuronal apoptosis and changes in expression of Bcl-2/Bax and caspase-3 in cerebral infarction rats through PTEN/PI3K/Akt signaling pathway. Exp Ther Med. 2020;19(3):2119-26.
77. Zhang CY, Ren XM, Li HB, Wei W, Wang KX, Li YM, et al. Effect of miR-130a on neuronal injury in rats with intracranial hemorrhage through PTEN/PI3K/AKT signaling pathway. Eur Rev Med Pharmacol Sci. 2019;23(11):4890-7.
78. Zheng T, Shi Y, Zhang J, Peng J, Zhang X, Chen K, et al. MiR-130a exerts neuroprotective effects against ischemic stroke through PTEN/PI3K/AKT pathway. Biomed Pharmacother. 2019;117:109117.
79. Ma Q, Li G, Tao Z, Wang J, Wang R, Liu P, et al. Blood microRNA-93 as an indicator for diagnosis and prediction of functional recovery of acute stroke patients. J Clin Neurosci. 2019;62:121-7.
80. Ni J, Wang X, Chen S, Liu H, Wang Y, Xu X, et al. MicroRNA let-7c-5p protects

against cerebral ischemia injury via mechanisms involving the inhibition of microglia activation. Brain Behav Immun. 2015;49:75-85.
81. Tian F, Yuan C, Hu L, Shan S. MicroRNA-93 inhibits inflammatory responses and cell apoptosis after cerebral ischemia reperfusion by targeting interleukin-1 receptor-associated kinase 4. Exp Ther Med. 2017;14(4):2903-10.
82. Zhang N, Zhong J, Han S, Li Y, Yin Y, Li J. MicroRNA-378 Alleviates Cerebral Ischemic Injury by Negatively Regulating Apoptosis Executioner Caspase-3. Int J Mol Sci. 2016;17(9).
83. Zhu G, Jiang L, Tan K, Li Y, Hu M, Zhang S, et al. MSCs-derived exosomes containing miR-486-5p attenuate cerebral ischemia and reperfusion (I/R) injury. Gene. 2024;906:148262.
84. Li D, Yang H, Ma J, Luo S, Chen S, Gu Q. MicroRNA-30e regulates neuroinflammation in MPTP model of Parkinson's disease by targeting Nlrp3. Hum Cell. 2018;31(2):106-15.
85. Denk J, Oberhauser F, Kornhuber J, Wiltfang J, Fassbender K, Schroeter ML, et al. Specific serum and CSF microRNA profiles distinguish sporadic behavioural variant of frontotemporal dementia compared with Alzheimer patients and cognitively healthy controls. PLoS One. 2018;13(5):e0197329.
86. Tan YJ, Wong BYX, Vaidyanathan R, Sreejith S, Chia SY, Kandiah N, et al. Altered Cerebrospinal Fluid Exosomal microRNA Levels in Young-Onset Alzheimer's Disease and Frontotemporal Dementia. J Alzheimers Dis Rep. 2021;5(1):805-13.
87. Zhou F, Zhang C, Guan Y, Chen Y, Lu Q, Jie L, et al. Screening the expression characteristics of several miRNAs in G93A-SOD1 transgenic mouse: altered expression of miRNA-124 is associated with astrocyte differentiation by targeting Sox2 and Sox9. J Neurochem. 2018;145(1):51-67.
88. Mullard A. NfL makes regulatory debut as neurodegenerative disease biomarker. Nat Rev Drug Discov. 2023;22(6):431-4.

Main tables and Figures

Table 1. Characteristics of patients at baseline

Characteristic	200mg x 2/day (N=3)	400mg x 2/day (N=3)	600mg x 2/day (N=2)	Total (N=8)
Sex, male	3 (100%)	3 (100%)	2 (100%)	8 (100%)
Age, years	67 (6.6), 60-73	60.3 (6.8), 55-68	69.5 (2.1), 68-71	65.1 (6.6), 55-73
Height, cm	179 (7.5), 171-185	163 (9.8), 152-172	174 (8.7), 168-180	172 (11.7), 152-185
Weight kg	73 (11), 62-84	83.9 (17.2), 66-100	78.8 (3.4), 76.4-81.2	78.6 (12.1), 62-100
Symptom duration, months	19.1 (6.5), 11.6-23.3	34.9 (33.4), 10.3-72.9	11 (0.4), 10.7-11.3	23 (21), 10.3 – 72.9
Diagnostic delay, months	11.3 (9.1), 8.3 – 19.3	14.5 (18.6), 2.9 - 36	9.4 (1.2), 8.5 – 10.3	12.2 (8.9), 2.9 - 36
El Escorial, definite	1 (33%)	1 (33%)	0	2 (25%)
Site of onset, bulbar	0	1 (33%)	2 (100%)	3 (38%)
Concomitant ALS medication use				
Riluzole only	2 (67%)	2 (67%)	2 (100%)	6 (75%)
Riluzole and Edaravone	1 (33%)	1 (33%)	0	2 (25%)
ALSFRS-R total score	31.3 (6.4), 24-36	32.3 (4.7), 27-36	38.5 (4.9), 35-42	33.5 (5.6), 24-42
ΔFRS, points per months	-1.1 (0.86), -2.1 – (0.54)	-0.95 (0.97), -2 – (-0.16)	-0.86 (0.42), -1.15 – (-0.56)	-0.97 (0.72), -2.1 – (-0.16)
FVC, % predicted	82.6 (27.2), 51.7-103	82.6 (17.6), 64-98.9	58 (1.4) 57-59	76.5 (20.8) 51.7-103
King's stage 2/3/4 (N)	1/1/1	1/1/1	0/1/1	2/3/3

Continuous data are presented with mean (standard deviation) and range, categorical data are presented as frequency (percentage).

ΔFRS = (48-ALSFRS-R total score)/ symptom duration.

Table 2. Overview of adverse events.

Dosing group	**200mg x 2/day (N=3)**		**400mg x 2/day (N=3)**		**600mg x 2/day (N=2)**	
Adverse event	**No of patients (%)**	**No of times reported**	**No of patients (%)**	**No of times reported**	**No of patients (%)**	**No of times reported**
Any adverse event	3 (100%)	13	3 (100%)	27	2 (100%)	12
Serious adverse event	0	0	0	0	0	0
Adverse event leading to discontinuation	0	0	0	0	1 (50%)	2
Severity						
Mild	2 (67%)	10	3 (100%)	16	2 (100%)	10
Moderate	1 (33%)	1	2 (67%)	10	1 (50%)	2
Severe	2 (67%)	2	1 (33%)	1	0	0
System organ class						
Nervous system	1 (33%)	1	2 (67%)	12	1 (50%)	3
Gastrointestinal	2 (67%)	6	2 (67%)	2	2 (100%)	8
Musculoskeletal	1 (33%)	2	2 (67%)	5		
Injury, poisoning and procedural complications	2 (67%)	2	1 (33%)	2		
General system disorders			2 (67%)	3	1 (50%)	1
Respiratory			1 (33%)	1		
Psychiatric			1 (33%)	2		
Vascular	1 (33%)	1				
Appetite	1 (33%)	1				
Related to drug	1 (33%)	5	2 (67%)	7	1 (50%)	7
System organ class Gastrointestinal						
Nausea	1 (33%)	4			1 (50%)*	3
Nervous system disorder						
Dizziness			1 (33%)	4	1 (50%)*	3
Headache			1 (33%)	2		
General system disorders						
Fatigue			1 (33%)	1		
Excess sweating					1 (50%)	1
Appetite						
Decreased appetite	1 (33%)	1				

*Increase in the severity of these AEs caused early termination.

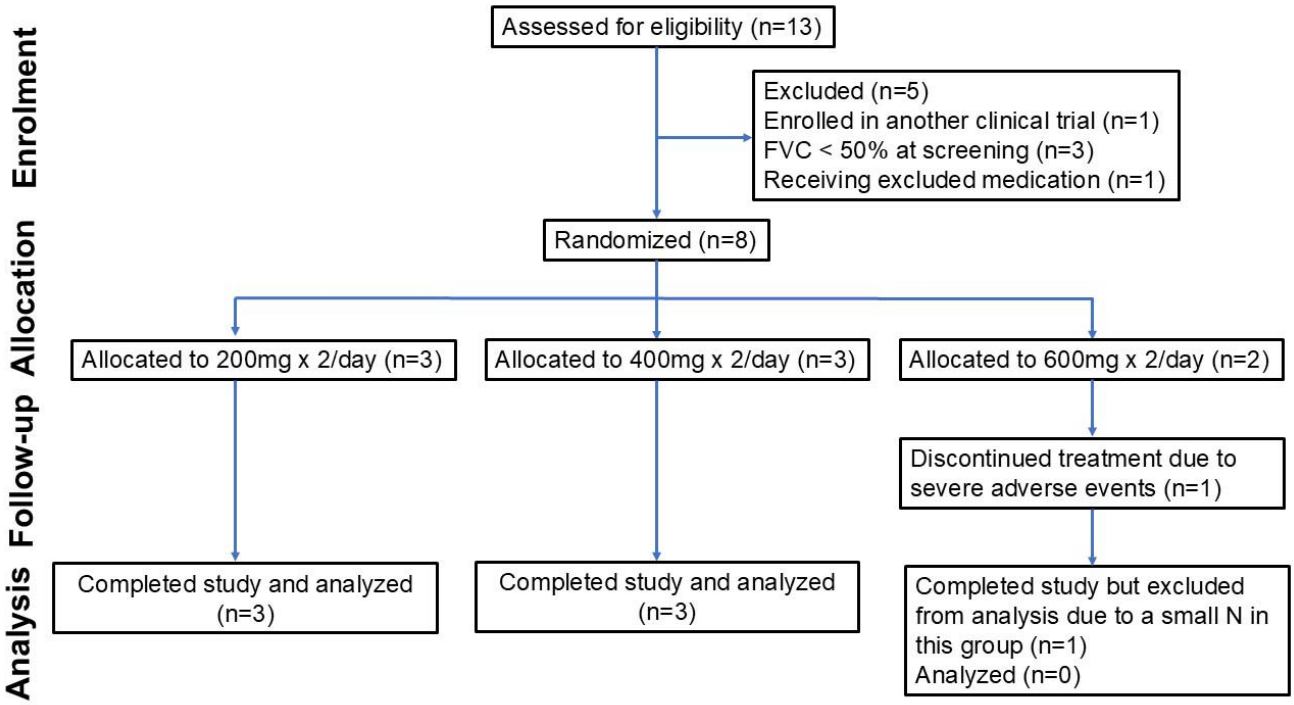

Figure 1. Flow diagram of the different stages of the REALS trial.

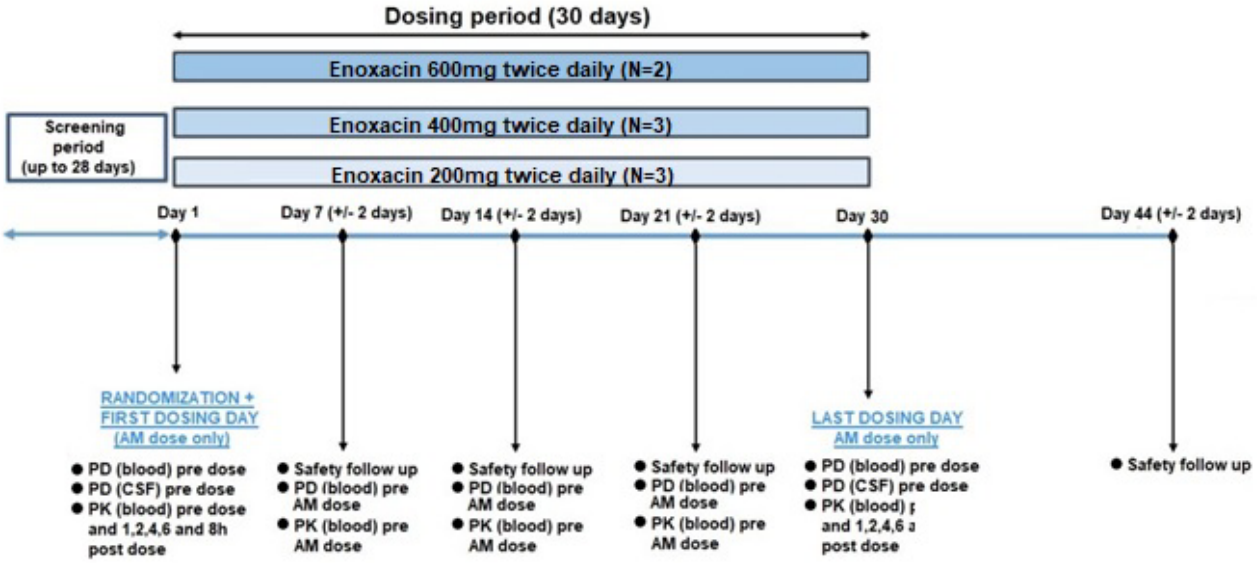

Figure 2. Illustration of study design. Dosing was performed over 30 days with a 14 days follow up for reporting adverse effects. Blood and CSF were collected pre-dosing (day 1). CSF was collected again on day 30. Blood was phlebotomized on days 7, 14, 21 and 30 with -/+ 2 days variation.

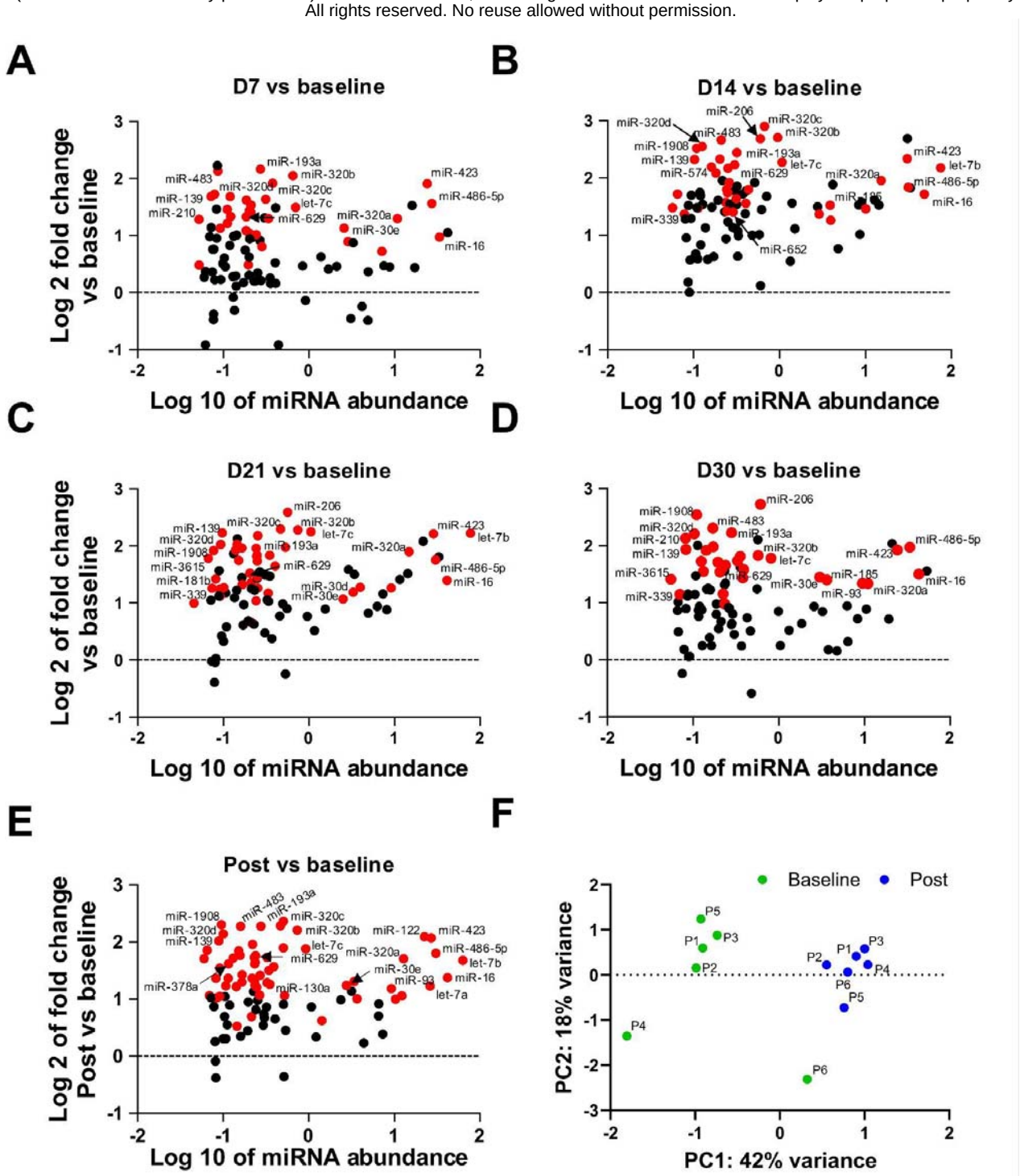

Figure 3. change in specific miRNA levels in the plasma, compared to baseline levels, on days 7 **(A)**, 14 **(B)**, 21 **(C)**, 30 **(D)** and in all four time points averaged, compared to baseline **(E)**. miRNA counts were corrected to patients and normalized to miR-451a levels. Log 2 transformed fold change (y-axis) is shown against Log 10 transformed mean miRNA abundance (x-axis). Red indicates miRNAs which are significantly changed vs baseline (FDR<0.1 after multiple hypotheses correction). **(F)** principal component analysis of data presented in E by individual samples. Dots are annotated with the patient number. Green/blue dots denote baseline /post-treatment samples. Data in panels A-D were analyzed with two-way repeated measure ANOVA, data in E were analyzed with multiple t-tests. Multiple hypothesis correction was performed by a Two-stage linear step-up procedure of Benjamini, Krieger and Yekutieli.

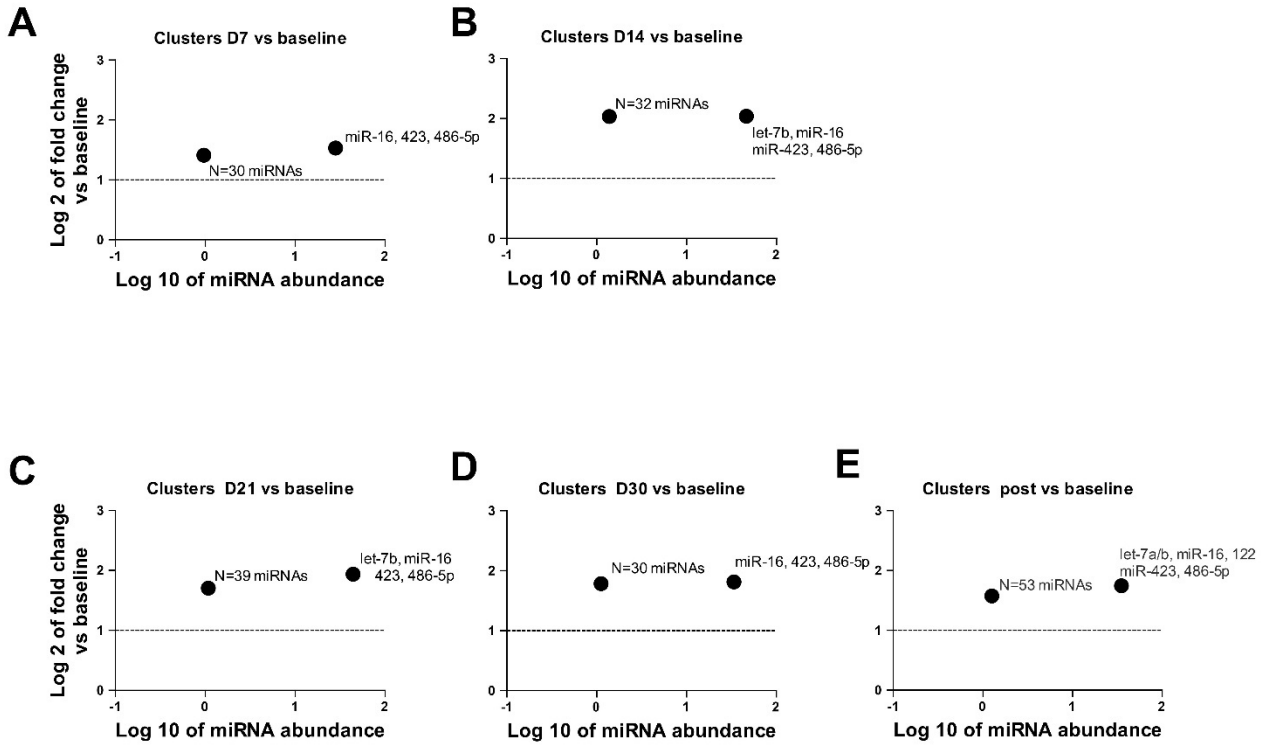

Figure 4. Centroids of k-mean clustering of changes in specific miRNA levels in the plasma, compared to baseline levels, on days 7 **(A)**, 14 **(B)**, 21 **(C)**, 30 **(D)** and in all four time points averaged, compared to baseline **(E)**. miRNA counts were corrected to patients and normalized to miR-451a levels. K-mean clustering was performed for the significantly increased miRNAs, with k=2 clusters. Log 2 transformed fold change (y-axis) is shown against Log 10 transformed mean miRNA abundance (x-axis). Next to each centroid are annotations, or number of the miRNAs included in the corresponding cluster.

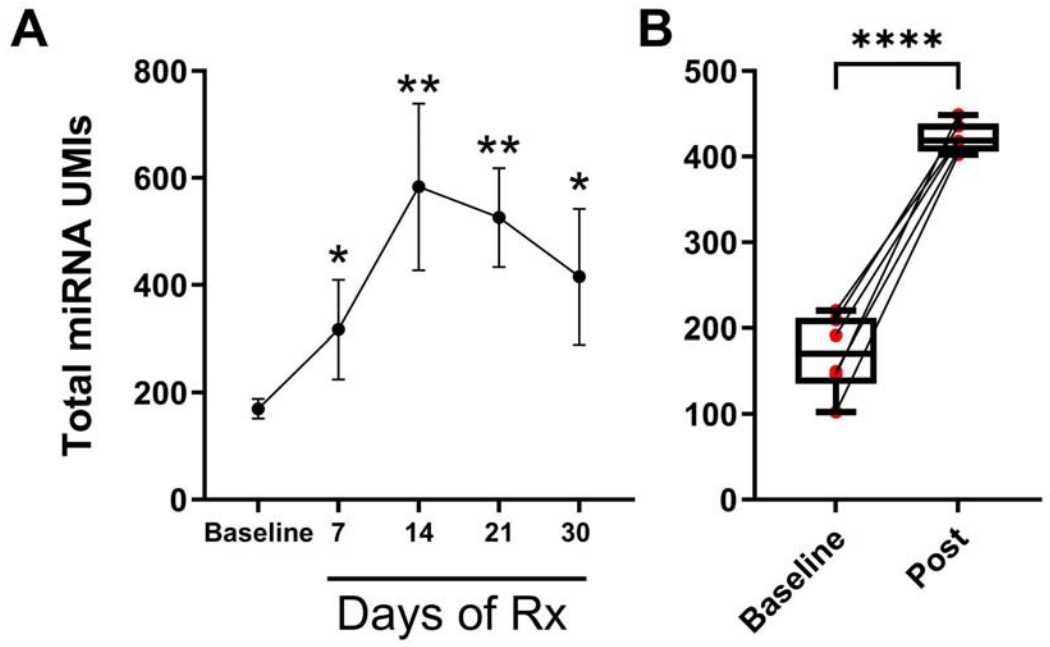

Figure 5. (A) Total miRNA levels, normalized by miR-451a levels in the plasma at baseline and on days 7, 14, 21 and 30 before morning dose (N=6 patients per time point). *FDR<0.1, **FDR<0.01 for comparisons vs baseline, Friedman test followed by Benjamini-Hochberg correction. **(B)** Total miRNA levels in the plasma, normalized to miR-451a, at baseline and post treatment (average of days 7, 14, 21 and 30). ***p<0.0001 vs baseline, paired t-test.

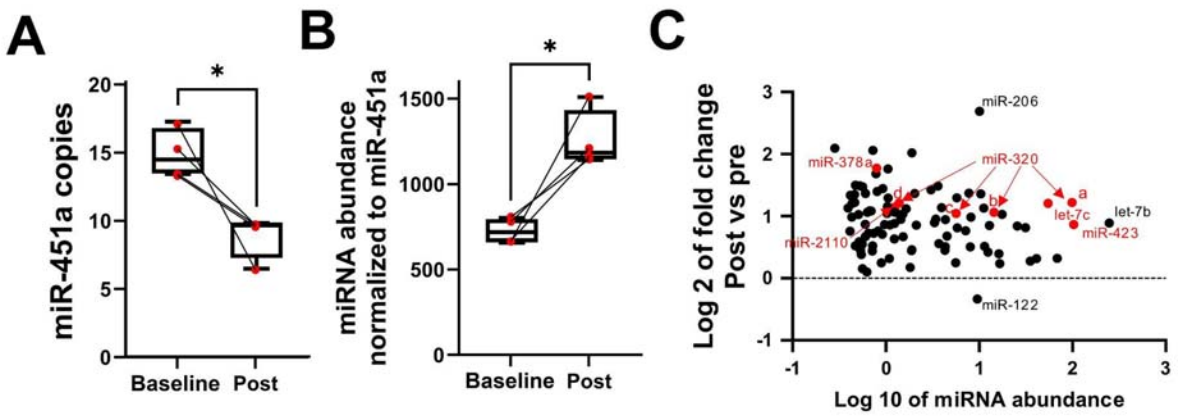

Figure 6. (A) CSF miR-451a decreases after Enoxacin treatment **(B)** Total CSF miRNA levels, normalized to miR-451a, in the CSF at baseline and at the completion of 1-month treatment with Enoxacin. *p<0.05, paired t-test. Data are presented as the mean ± SEM of four patients per time point. **(C)** change in specific miRNA levels after 1-month treatment compared to baseline levels. miRNA counts in each sample were corrected to patients and normalized to the corresponding levels of miR-451a. Log 2 transformed fold change (y-axis) is shown against log 10 transformed mean miRNA abundance (x-axis). Red indicates significantly changed miRNAs (FDR < 0.1, multiple paired t-test followed by the two-stage linear step-up procedure of Benjamini, Krieger and Yekutieli). miR-320 family members are shown with their suffix letter (a, b, c, d) next to the data point.

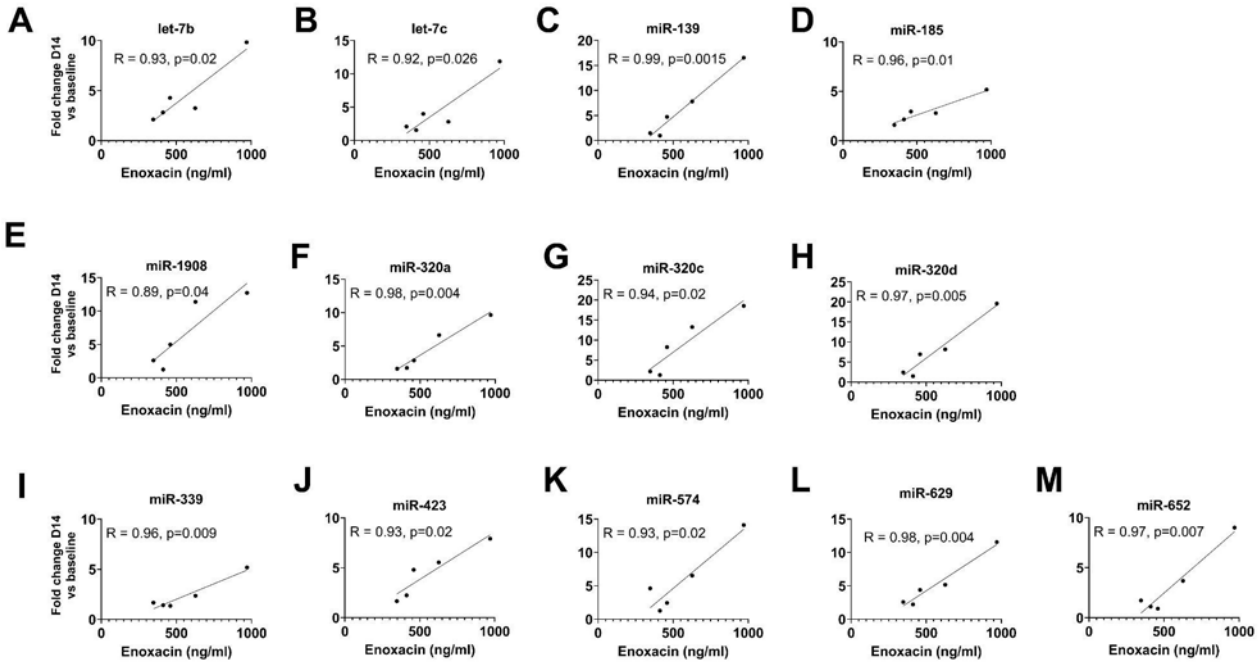

Figure 7. Pearson correlation between Enoxacin levels and fold-change values of miRNAs measured on day 14. p-values shown are unadjusted. All p-values displayed an FDR<0.1 after Benjamini-Hochberg correction.

Supplementary tables and figures

C_{trough} (ng/ml)				C_{max} (ng/ml)		t_{max} (hr)	
Day 7	**Day 14**	**Day 21**	**Day 30**	**Day 1**	**Day 30**	**Day 1**	**Day 30**
628 (286)	563 (250)	548 (288)	685 (296)	1324 (477)	1752 (475)	2 (1.1)	2 (1)

Supplementary table 1. Pharmacokinetic parameters of Enoxacin in plasma: trough concentrations on days 7, 14, 21 and 30 before morning dose, maximal concentrations and time to reach maximal concentrations on days 1 and 30 after Enoxacin morning dose. Data are presented as mean (sd).

Riluzole concentration (ng/ml)

Day 1				**Day 30**			
2h	**4h**	**6h**	**8h**	**2h**	**4h**	**6h**	**8h**
93.53 (35.7)	82.4 (31.7)	78.0 (36.7)	66.67 (34.1)	237.3** (84.4)	209.3* (96.7)	177.8* (99.1)	156.7* (90.6)

Supplementary table 2. Plasma Riluzole concentrations on days 1 and 30 at the indicated times after Enoxacin morning dose. Data presented as mean (sd). *FDR<0.05, **FDR<0.01 compared to the respective hour on day 1, repeated measure ANOVA followed by Benjamini-Hochberg correction.

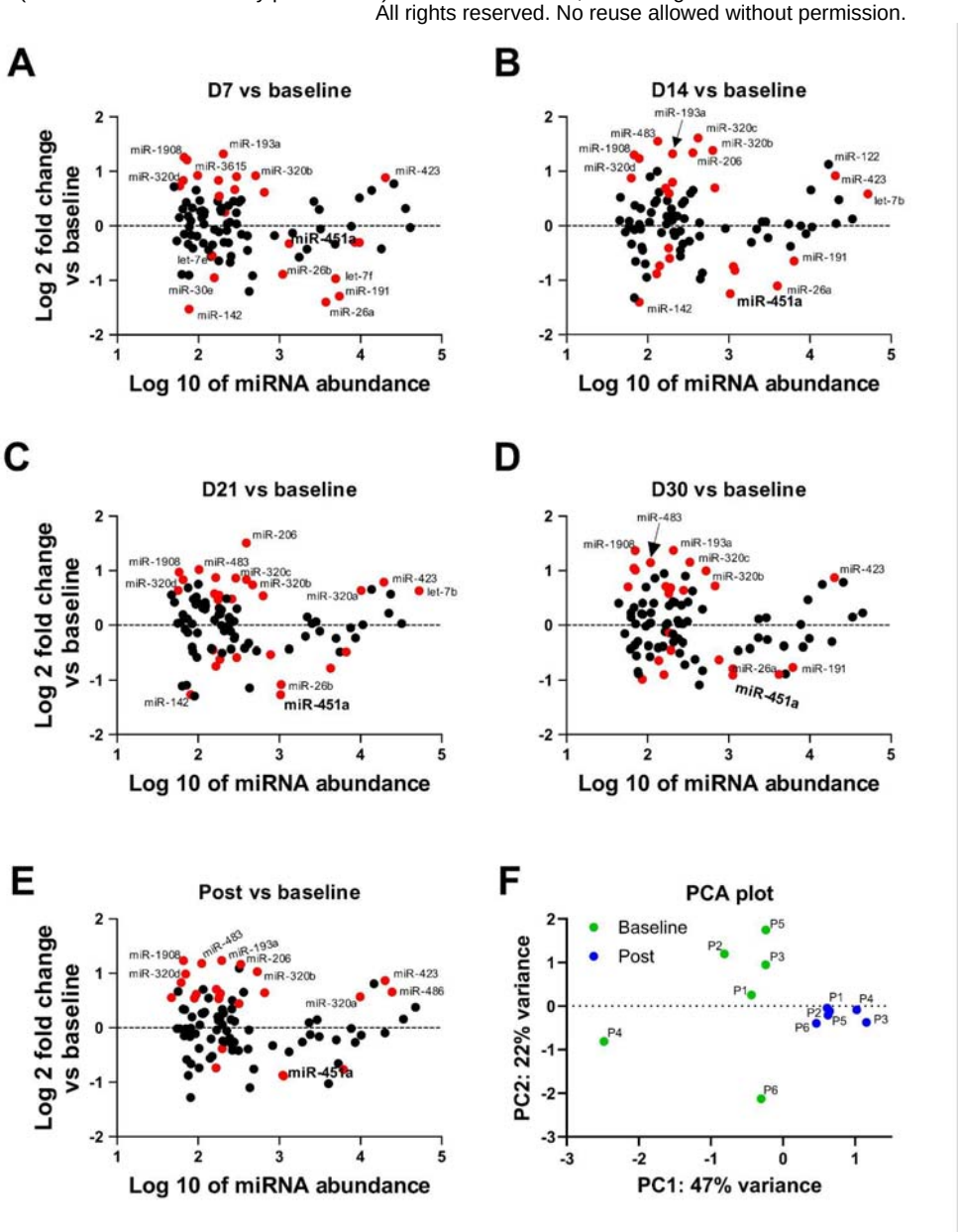

Supplementary figure 1. change in specific miRNA levels in the plasma, compared to baseline levels, on days 7 **(A)**, 14 **(B)**, 21 **(C)**, 30 **(D)** and in all four time points averaged, compared to baseline **(E)**. miRNA counts were corrected to patients and normalized to size factor by DESeq2. Log 2 transformed fold change (y-axis) is shown against Log 10 transformed mean miRNA abundance (x-axis). Red indicates miRNAs which are significantly changed vs baseline (FDR<0.1 after multiple hypotheses correction). **(F)** principal component analysis of data presented in E by individual samples. Dots are annotated with the patient number. Green/blue dots denote baseline/post-treatment samples. Data presented in panels A-D were analyzed with two-way repeated measure ANOVA. Data in E were analyzed with multiple t-tests. Multiple hypothesis correction was performed by a Two-stage linear step-up procedure of Benjamini, Krieger and Yekutieli.

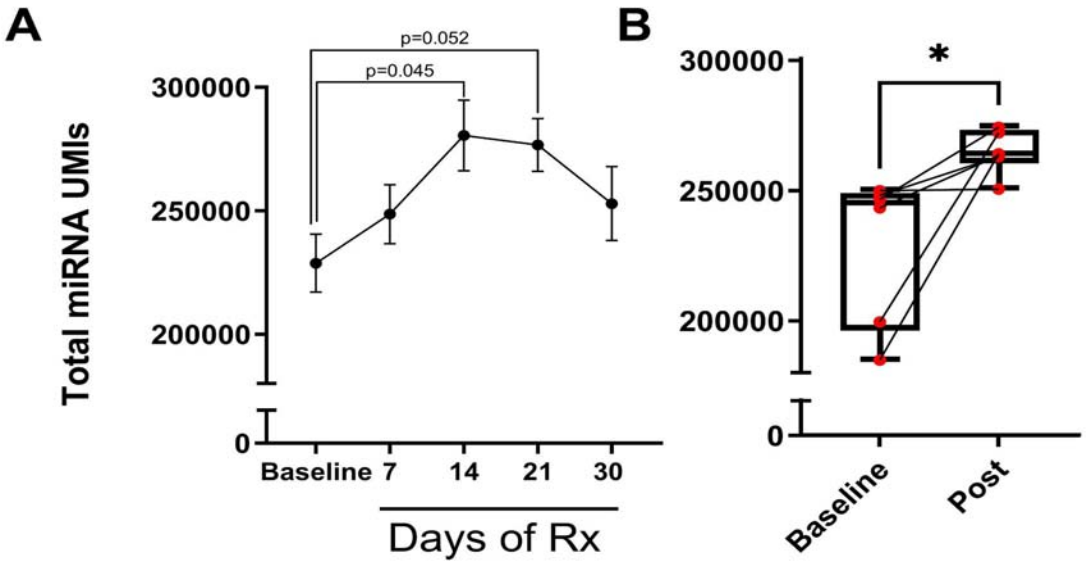

Supplementary figure 2. (A) Total miRNA levels, normalized by DESeq2 in the plasma at baseline and on days 7, 14, 21 and 30 before morning dose (N=6 patients per time point). P-values for individual paired t-test comparisons vs baseline are shown **(B)** Total miRNA levels in the plasma, normalized by DESeq2, at baseline and post treatment (average of days 7, 14, 21 and 30). *p<0.05 vs baseline, paired t-test.

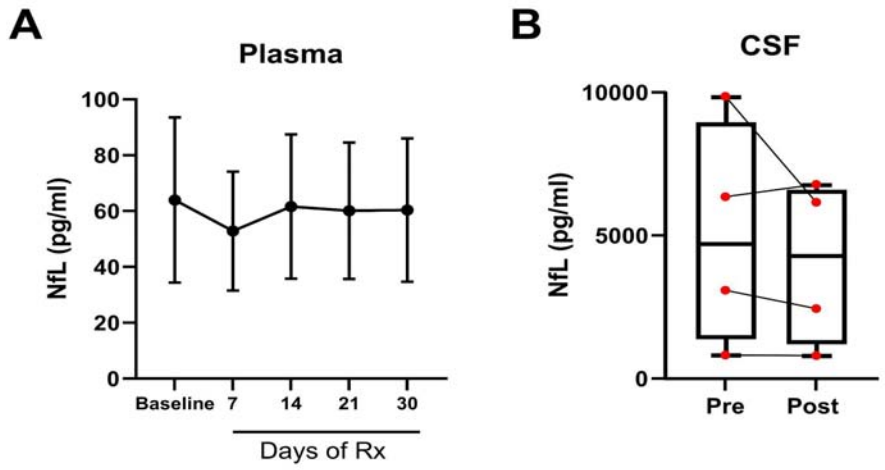

Supplementary figure 3. NfL levels measured in plasma **(A)** and CSF **(B)**. Enoxacin did not affect NfL levels in plasma (one-way repeated measure ANOVA: p=0.27), or in the CSF (p=0.37, paired sample t-test).